Microseismicity and faulting in the southwestern Okinawa Trough

Jing-Yi Lin [a,e,*], Jean-Claude Sibuet [a], Chao-Shing Lee [b], Shu-Kun Hsu [c], Frauke Klingelhoefer [a], Yves Auffret [a], Pascal Pelleau [a], Jacques Crozon [a], Cheng-Horng Lin [d]

[a] Ifremer, Centre de Brest, BP 70, 29280, Plouzané, France
[b] Institute of Applied Geophysics, National Taiwan Ocean University, Keelung, Taiwan
[c] Institute of Geophysics, National Central University, Chung-Li, Taiwan
[d] Institute of Earth Sciences, Academia Sinica, P. O. Box 1-55, Nankang, Taipei, Taiwan
[e] Collège de France, Chaire de Géodynamique, Européle de l'Arbois, Bat. Le Trocadéro - Aile Sud, BP 80, 13545 Aix en Provence cedex 4, France

Abstract

In November 2003, 15 ocean bottom seismometers were deployed in the southwestern Okinawa Trough. More than 3300 microearthquakes were located during the 10-days passive seismic experiment. The earthquake activity is characterized by the ceaseless occurrence of small earthquakes in the vicinity of all the instruments. The seismicity is essentially restricted to the central part of the Southwestern Okinawa Trough, except for one cluster of events situated in the southern part of it (cluster 2). The seismic activity terminates abruptly against the NE–SW trending prolongation of the Lishan fault. Most of the microearthquakes are aligned along the E–W trending normal faults, showing where the present-day active normal faulting occurs and how it accounts for the N–S extension in the Okinawa Trough. According to the P-wave velocity spectra estimated from some deep earthquakes located beneath the cross backarc volcanic trail area, the existence of a lower crustal/upper mantle magma chamber is confirmed by the presence of low frequency earthquakes in the 3–10 Hz bandwidth.
© 2008 Published by Elsevier B.V.

1. Introduction

The Okinawa Trough (OT) is a continental backarc basin currently opening behind the Ryukyu arc-trench system where the Philippine Sea plate (PH) subducts beneath the Eurasia plate (upper inset in Fig. 1). It can be considered as a complex area in which numerous geodynamic features interfere (backarc features, volcanic front, abnormal volcanism linked to the 123°E slab tear, previous geological trends). Refraction data acquired in the Okinawa Trough reveal that the crust is of continental origin and the crustal thickness along the trough axis increases from 15–18 km in the southern OT to 27–30 km in the northern OT (Lee et al., 1980; Iwasaki et al., 1990; Hirata et al., 1998; Sibuet et al., 1995). Based on the swath-bathymetric and seismic data, numerous normal faults were mapped by Sibuet et al. (1998) allowing to identify the two last phases of extension in the

southwestern Okinawa Trough (SOT) with N150° directions of extension during the Pleistocene (2–0.1 Ma) and N170° during the late Pleistocene–Holocene phase of extension (0.1–0 Ma). The direction of present-day extension, estimated from the focal mechanism solutions of earthquakes occurring in the axis of the SOT, commonly strikes within 30° of the N–S direction (Dziewonski et al., 1981; Fournier et al., 2001; Kubo and Fukuyama, 2003). Two databases of GPS measurements in the Taiwan region (Yu et al., 1995 and 1997) and in the southern Ryukyu Arc (Heki, 1996; Imanishi et al., 1996) were combined by Lallemand and Liu (1998). These movements are relative to the South China Sea. The westernmost part of Ryukyu Arc, Yonaguni Island, is moving southward with a velocity 1.4 cm/yr faster than the north of Taiwan (Ilan Plan) which accounts for the Okinawa Trough opening processes. The volcanic front (dotted gray line in Fig. 1) extends from Japan to Taiwan. From Kyushu to Okinawa Island, it follows the active volcanoes of the Ryukyu Arc and progressively migrates inside the OT, following small subaerial active volcanoes located about 25 km west of the non-volcanic
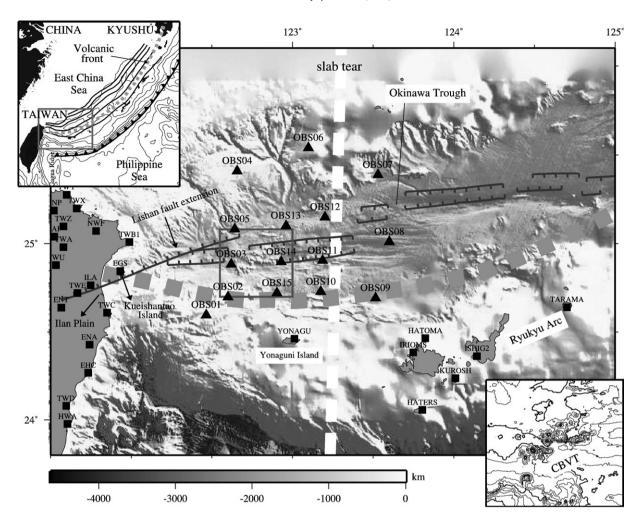

Fig. 1. Shaded bathymetry in the northwestern corner of the Philippine Sea plate extracted from Sibuet (in prep.). The location of the Lishan fault extension and Okinawa Trough normal faults are from Sibuet and Hsu (2004). Locations of the 15 OBS (black triangles) used during the 2003 experiment and surrounding land stations (black squares). The white dashed line shows the location of the slab tear (Lin et al., 2004a and b). In the upper left corner, the general map of the Ryukyu subduction zone with slab depths every 50 km and location of the volcanic front (dashed line). In the lower right corner, detailed bathymetry (isobathic spacing, 100 m) of the cross backarc volcanic trail (CBVT) (Sibuet et al., 1998) located in the gray square box.

arc. Southwest of Okinawa Island, it migrates inside the OT, follows numerous seamounts associated with high amplitude magnetic anomalies (Hsu et al., 2001), then cuts across the cross backarc volcanic trail (CBVT), which consists of a cluster of about 70 seamounts located west of 123°E longitude (lower inset in Fig. 1) and finally ends 10 km offshore of Taiwan in Kueishantao Island (Sibuet et al., 1998; Chung et al., 2000). According to seismicity data (Engdahl et al., 1998) and depths of magnetic basement (Lin et al., 2004a), a slab tear was identified along the 123.2°E meridian (Fig. 1). Based on Vp, Vs and Vp/Vs tomographic images, an excess of partial melting identified along the slab tear is at the origin of the abnormal CBVT volcanism (Lin et al., 2007). The Lishan fault is a major feature of Taiwan, which separates the Hsuehshan Range from the Backbone Range (Ho, 1986; Lee et al., 1997). It continues in the Ilan Plain (Hsu et al., 1996) and in the westernmost part of the SOT and was identified up to 122.6°E longitude (Sibuet et al., 1998). Its existence was suspected east of 122.6°E but not firmly established due to the lack of seismic reflection data. The Lishan fault and its OT prolongation seem to be a major crustal or even lithospheric

feature which offset the tensional features of the SOT and Ilan Plain.

Thus, the SOT is located in a complex geologic setting that can be better understood if we are able to constrain its deep crustal structure. As this region is a seismically active area, the idea is to look at the hypocenter distribution in order to better understand the geological context. In the past, the SOT seismicity was established by using only land seismic stations recordings. The depth accuracy of offshore seismic activity analyzed from existing land data was often poor, even if seismological data from the two Taiwanese and Japanese networks of land stations are coupled (Hsu, 2001; Nakamura et al., 2003). Because of this limitation, a passive ocean bottom seismometer (OBS) experiment performed in this area is a good way to increase the resolution of earthquake data.

2. Data acquisition

The passive seismic OBS experiment was conducted from November 19 to December 1, 2003. 15 OBSs were deployed in
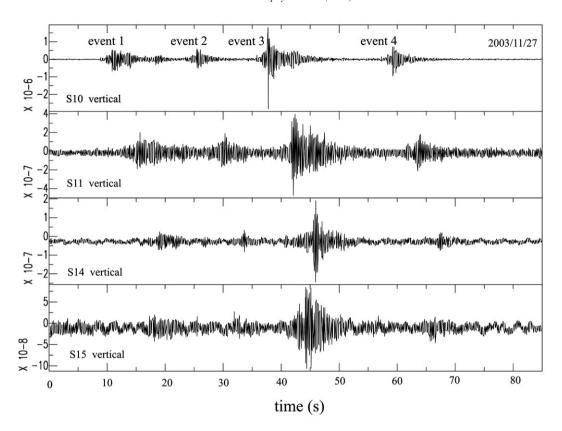
Fig. 2. Example of microearthquakes recorded on the vertical channel seismograms of 4 stations, showing the large number of recorded earthquakes. At least four events are identified during 1 min.

a 130×90 km area including the Ryukyu slab tear (Lin et al., 2004a and b) and the CBVT (Sibuet et al., 1998) (Fig. 1). The spacing between OBSs varied from 15 to 40 km. The OBSs were equipped with three 4.5 Hz component geophones and one broad-band type hydrophone (Auffret et al., 2004).

Seismic events were detected manually on continuous seismic records. Data of stations OBS01, OBS02, OBS04, OBS05 and OBS06 are noisy, probably because they were deployed in shallow water depths (about 400 m), where the signal is polluted by the sea-surface waves, especially during the winter monsoon season. For all OBSs, most of the seismic events are weak and only recorded by one OBS. The number of recorded events rises up to 50 events/hour (Fig. 2). Many events do not have sufficient magnitude to be recorded on 3 or more OBS stations excluding the possibility to determine their hypocenters. Localized earthquakes often cluster both in time and space (Fig. 2) with daily frequencies of events varying from 250 to 600.

To accurately locate the microearthquakes, the _HYPOCENTER_ method (Lahr, 1978; Lienert et al., 1988) is used. This method is based on the calculation of root mean square (rms) travel time residuals. Arrival times of P and S waves are used for the hypocenter determination. A 1-D P wave velocity model calculated from tomographic data of Nakamura et al. (2003) is used as a reference (Fig. 3), and the Vp/Vs ratio is assumed to be 1.73. The magnitude of earthquakes was evaluated by using the duration of seismic waves (hereafter named Md; Tsumura, 1967). Although more than 5000 events were identified on a single OBS,
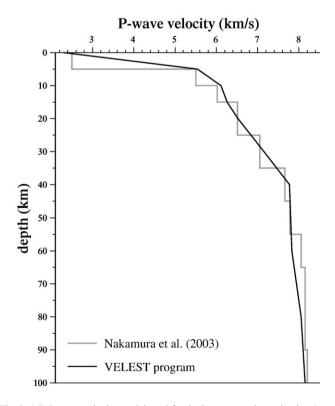

Fig. 3. 1-D P-wave velocity model used for the hypocenter determination (gray line) by Nakamura et al. (2003) and 1-D best-fit velocity model derived by using the VELEST program (black line)(Kissling et al., 1994). Vp/Vs is assumed to be 1.73.

only 3300 events were successfully located. The horizontal and vertical error of the hypocenter determination is 3.18 and 6.58 km respectively. The high microseismic activity suggests that the crust is highly and continuously fractured, as it was already highlighted by the presence of numerous normal faults identified in this area (Sibuet and Hsu, 1997 and 2004; Sibuet et al., 1998).

We also used events recorded by land stations (Central Weather Bureau (CWB) in Taiwan and Japan Meteorological Agency (JMA), Fig. 1) throughout the OBS recording period in order to increase the precision of the hypocenter determination. In total, more than 20 events of magnitude >3 were recorded simultaneously by the three networks (CWB, JMA and OBSs) during the recording period. Most of the microearthquakes occurring in the SOT were not detected on land stations, while many small magnitude earthquakes which occurred along the deep seismic zones or above were well recorded. Small magnitude events are difficult to detect at great distances because of the high attenuation of seismic waves in the Okinawa Trough as already demonstrated by an OBS experiment coupled with land stations recording in the middle OT (Ouchi and Kawakami, 1989). The origin of this high attenuation could be also linked to a low-Q material determined in the Okinawa Trough where high heat flow values were found (Yamano et al., 1986). Therefore, the lack of microearthquakes recorded on land stations, the high heat flow values and the high volcanic activity in our study area (Tsai et al., 1998; Shyu and Liu, 2001) might suggest a mechanism similar to the low-Q structure in the middle OT area (Ouchi and Kawakami, 1989).

3. Earthquakes relocation and hypocenter distribution

3.1. Method

In this study, the best-fit 1-D model was derived using the VELEST program, which simultaneously inverts arrival times for 1-D velocity structure, station corrections and hypocenters (Kissling et al., 1994). The obtained 1-D P-wave velocity model is broadly similar to our reference 1-D velocity model (Nakamura et al., 2003) (Fig. 3). The calculated station corrections are very small (<0.17 s) with exceptions for stations with a few observations (Table 1). Surprisingly, for stations located in the central SOT graben (OBS8, OBS11 and OBS14 in Fig. 1) where the sedimentary thickness is about 1 km, the station corrections are negative and very small (about-0.05 s). However, for the stations situated just north of the Ryukyu Arc, beneath the volcanic front (OBS09, OBS10 and OBS15 in Fig. 1), high station corrections were determined. This is probably due to the presence of volcanic outcrops located in the SOT axis, which lowers the delay with respect to areas where sediments are present.

Because the seismic velocity structure strongly varies perpendicularly to the subduction zone, a 1-D seismic velocity structure is not sufficiently accurate for a precise hypocenter determination. A 3-D velocity model is required to obtain more precise hypocenter locations. In addition, the use of a constant Vp/Vs ratio for hypocenter determinations can be problematic as the hypocenter depth determinations largely depend on Vp/Vs ratios (e.g. Obana et al., 2001). In a complex geological environment, a realistic Vp/Vs structure must be used to accurately determine hypocenters. We therefore used the *simul2000* program (Thurber and Eberhart-Phillips, 1999), which allows for true stations elevations and relocating earthquakes with a 3-D P-wave velocity and Vp/Vs model. The layered model from the best VELEST solution was used as the starting 1-D model and a minimal grid spacing of 15 km is used for the simul2000 program. To obtain a better 3-D velocity model and also a better determination of hypocenters, only events located with an error of hypocenter determination less than 10 km in the three directions were selected for the relocation. In total, 2823 earthquakes were relocated in this study. After the relocation, the average rms residual decreases from 0.242 to 0.151 s, showing a better determination of hypocenters.

3.2. Hypocenter locations

After relocation, some events were shifted as much as 35 km horizontally and 25 km in depth. Cluster of events are better defined, which shows the effectiveness of the relocation. Most of the earthquakes are now clustered and aligned along the axis of the SOT. The seismicity in the SOT appears to be quite complex, and microearthquakes are widely distributed over the whole area (Fig. 4). 80% of the earthquakes are shallower than 20 km which means that most of the recorded earthquakes have a crustal origin. The earthquakes can be divided into three groups: those occurring in the trough, those occurring along the deep subduction plane, which were generally recorded by the three seismic networks, and those linked to other geological features (e.g. lateral compression seismic zone; Kao et al., 1998). Concerning the earthquakes located in the trough, four major clusters are observed (Fig. 4): (1) in the CBVT area, located in the axis of the SOT (24.7–25°N; 122.45–122.98°E); (2) in the southern part of the SOT (24.6–24.85°N; 123.05–123.35°E); (3a) further east in the axis of the OT (24.9–25.05°N; 123.05–123.48°E) and (3b) northeast of cluster 3a (25.1–25.35°N; 123.15–123.8°E), near the northern OT continental slope. Most of the events in clusters 1 and 2 are shallow (less than 20 km). Less shallow earthquakes with small magnitude are observed in the two last clusters probably due to the larger distance between OBS stations. An en-échelon shape of earthquake distributions is observed (Fig. 5), similarly to the

Table 1
Summary of station corrections (only for OBS)

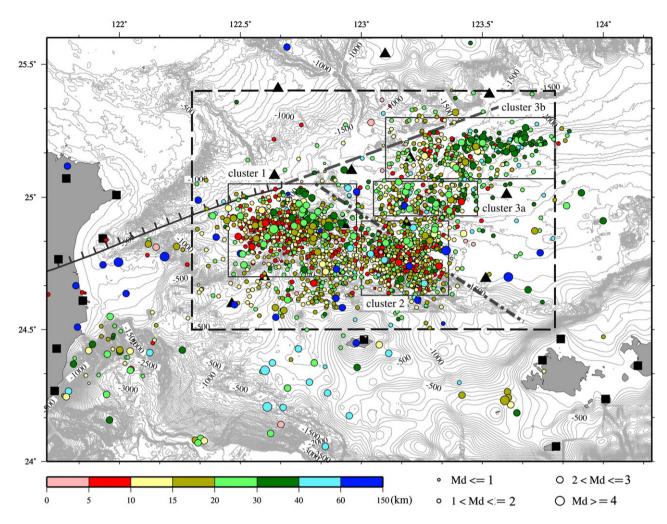| Station	S01	S02	S03	S04	S05	S06	S07	S08	S09	S10	S11	S12	S13	S14	S15
P (s)	0.17	0.113	−0.118	0.000	−0.139	−0.047	−0.131	−0.041	0.031	0.167	−0.052	−0.055	−0.082	−0.158	0.117
S−P (s)	−0.063	−0.027	0.036	0.000	0.115	−0.054	−0.005	0.050	0.063	−0.068	0.030	−0.020	0.100	0.121	−0.115

Fig. 4. Hypocenters of 2833 microearthquakes relocated with the simul2000 program (Thurber and Eberhart-Phillips, 1999) in the southwestern Okinawa Trough during the 10-days acquisition period. The dashed square shows the location of Fig. 5. Four small rectangles delineate the four earthquake clusters (1, 2, 3a and 3b). The size of dots is function of the magnitude. Colors show the different depth ranges of earthquake. Bathymetric contours every 100 m (Sibuet and Hsu, 2004). The dashed line is the prolongation of the Lishan fault. Black triangles correspond to the locations of OBS stations and black squares to surrounding land stations.

pattern of hypocenter locations reported by Sato et al. (1994) in the middle OT, west of Okinawa Island. Many microearthquakes are distributed along E–W trending normal faults already identified in the SOT area (Fig. 5), indicating which normal faults are active in the SOT. Earthquakes are less numerous in clusters 3a and 3b, and their depths range is 0–40 km. The 20–40 km deep earthquakes are too deep to be crustal earthquakes. However, an E–W lineament of hypocenter distribution is found for these two clusters (Fig. 5). Therefore, the extension stress field does not seem to be only restricted to the crust, but extends to the upper mantle.

3.3. Informations from land seismic networks

In order to show the input of an OBS experiment in the SOT area, we have compared the earthquakes located by the three networks (CWB, JMA and OBS networks, Fig. 6). To better illustrate the distribution of hypocenters associated with the normal faulting and related activities, all the earthquakes presented in Fig. 6 are shallower than 60 km.

3.3.1. Central Weather Bureau data

The present-day CWB network consists of 77 seismic stations located in Taiwan Island. During the 1996–1999 period, 18,563 earthquakes of magnitude larger than 1 were located by the CWB network in our study area. Because all stations are land stations, the earthquake locations were restricted by the CWB to the west of 123°E (Fig. 6a) (e.g. Tsai and Wu, 1996; Kao et al., 1998) even if we know that the geographical locations and depths of earthquakes are poor far from Taiwan. Many former studies of the distribution of earthquakes in Taiwan have been carried out (e.g. Tsai, 1986; Wang et al., 1994), and the seismicity in northeastern Taiwan is delineated by several groups (e.g. collision seismic zone, lateral compression zone, etc; Kao et al., 1998). One of the most obvious cluster is the Okinawa Trough seismic zone which trends in the E–W direction and is situated near the axial center of the Okinawa Trough along a 110-km-long segment lying from the Ilan Plain in northeastern Taiwan to longitude 122.6°E (Kao et al., 1998; Font et al., 1999). The depth range of this cluster is 0–40 km. The cluster is further divided into two
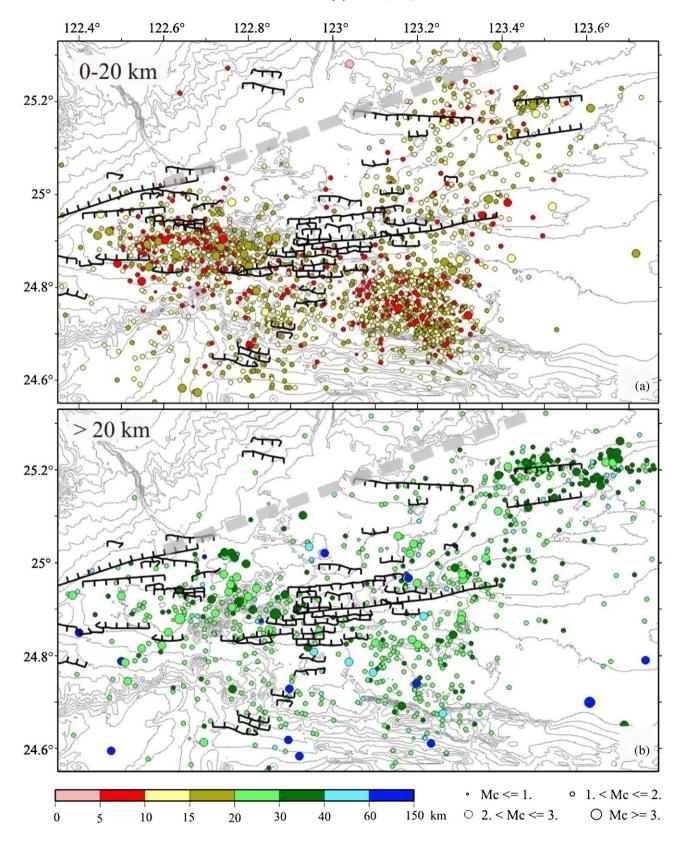
Fig. 5. Hypocenters distribution for two depth ranges (in the framework located in Fig. 4). (a) 0 to 20 km; (b) more than 20 km. The location of normal faults is from Sibuet et al. (1998) and Sibuet and Hsu (2004). Dots are the hypocenter positions. The dashed line is the prolongation of the Lishan fault.

seismic belts (gray dashed contours in Fig. 6a). The northern belt starts a few kilometers east of the Ilan Plain and lies along the 24.8°N parallel, roughly in the E–W direction, in the axis of the trough between 121.9 and 122.6°E. The southern belt trends along the 24.7°N parallel, on the northern slope of the Ryukyu Arc, between 122.2 and 122.6°E (Wang et al., 2000; Font, 2002).

The northern belt corresponds approximately to cluster 1 recorded by the OBS network (Figs. 6a and c). The hypocenter distribution is located south of the Lishan fault prolongation and east of Ilan Plain. The prolongation of the southern belt might be connected to cluster 2 recorded by the OBS network (Fig. 6c). However, as there is no seismicity located by the CWB network east of 123°E, this point has to be confirmed by further observations.
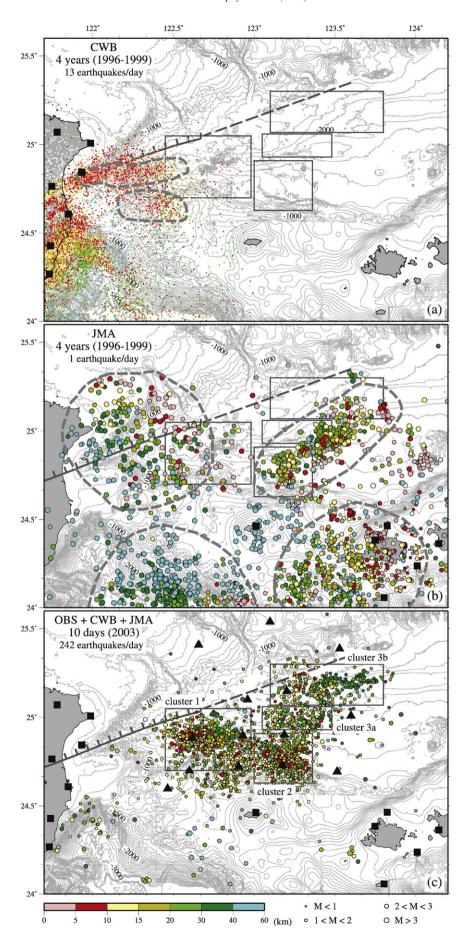
3.3.2. Japan Meteorological Agency data

The JMA seismic network includes more than 350 seismic stations distributed over the Japanese islands. The earthquakes located in our study area are mainly recorded by the 7 westernmost stations of the JMA network, which are installed on the Ryukyu Arc islands (Figs. 1, 6b and c). During the 1996–1999 period, 1891 earthquakes ($M > 1$) were located by the JMA network in our study area. Earthquakes are concentrated into four groups (gray dashed contours in Fig. 6b) with two of them on each side of the 122.9°E meridian and rather symmetrical with respect to this line. The southern two groups correspond to intraplate earthquakes located beneath the Ryukyu Arc slope and Nanao Basin, west of the 122.9°E, and beneath the upper sedimentary Ryukyu forearc, east of 122.9°E. The northern two groups belong to the Okinawa Trough area and correspond to crustal backarc extensional mechanisms (e.g. Kao et al., 1998). The northwestern cluster was not detected by the much closer to the source Taiwanese network and does not appear in the global seismicity data (e. g. Engdahl et al., 1998). We consider that this cluster of events is mislocated and must be moved toward the southeast, belonging thus to the seismicity situated in the Okinawa Trough seismic zone. The northeastern cluster is also identified by our OBS network (clusters 2, 3a and 3b in Figs. 6b and c), globally lying along a NE–SW trend. Earthquakes determined by the JMA network present larger magnitudes than those located by the OBS network and are globally located 10-km south of clusters 2, 3a and 3b. As these earthquakes are outside of the JMA network, we consider that the northeastern JMA cluster might be due to mislocation and must be moved westward as already mentioned by Nakamura and Katao (2003). However, the earthquakes are distributed approximately along the NE–SW direction parallel to the prolongation of Lishan fault.

3.3.3. Data recorded by the three networks (OBS+ CWB+ JMA)

2422 earthquakes of magnitude higher than 1 and depths shallower than 60 km were located by the OBS network during the 10-days period in 2003. The daily frequency of more than 240 events is surprisingly high compared to the daily number of events recorded in this area by the two land seismic networks. This is due to the fact that the OBS network recorded a majority of earthquakes of magnitude <3. As mentioned above, normal faulting is the main factor controlling the tectonic activity in the SOT area. The E–W trending earthquake distributions are observed in the three clusters located in the axis of the SOT (clusters 1, 3a and 3b) (Fig. 5). Although we can faintly recognize the corresponding clusters from the distributions of events located by the land network, there is a large uncertainty concerning the locations of these clusters, due to the limited azimuthal coverage of land stations. Thus, it is not easy to properly determine the relationship between seismicity and tectonic trends. The OBS experiment plays an important role in the identification of the sources of microseismicity and also in the increase of accuracy of hypocenter determinations in the SOT area.

3.4. Tectonic boundaries suggested by the microseismicity distribution

The main seismicity is concentrated in the central part of the SOT and not outside because the seismic stations are located all around the area of significant seismicity. In the north, the hypocenter distribution terminates abruptly against the prolongation of the Lishan fault (gray dashed line in Fig. 4). Sibuet et al. (1998) already suggested that the Lishan fault extension is the boundary between the Eurasia plate and the Okinawa platelet. According to the hypocenter distribution, the Lishan fault prolongation could be extended in the northeast direction until the 123.6° meridian. North of this boundary, only a few earthquakes were detected. On the other hand, it should be noticed that only a few earthquakes are located in the area between the deep graben depression of the SOT and Taiwan Island, despite the fact that the OBS network is coupled with the CWB network (Fig. 4). We confirm the observations of Kao et al. (1998) and Font (2002) concerning the distributions of relocated earthquakes. To the west, the seismicity of the SOT drops away 30 km east of Ilan Plain. This might suggest that backarc rifting processes are less active in this area than in the graben depression of the SOT. Several studies suggest that northeast Taiwan is affected by the extensional process of Okinawa Trough (e.g. Yeh et al., 1989; Liu, 1995; Kao and Rau, 1999; Kao and Jian, 2001). Thus, the absence of small magnitude seismic activity near and east of the Ilan Plain with respect to the SOT area does not mean that backarc rifting process ceases west of the Lishan fault but that the Lishan fault extension plays an important role by disrupting the normal faulting activity on each side of this boundary. The Lishan fault separating two major geologic units inland Taiwan is considered to be a former suture zone between the Chinese continental margin and an accretionary prism (Lu and Hsü, 1992; Lee et al., 1997) or to be a suture zone between the continental margin and a sliver of continental lithosphere (Shyu et al., 2005). As a result, this structure and its prolongation might change the stress

---

Fig. 6. (a) 18,570 hypocenters located by the Central Weather Bureau (CWB) network by using Taiwanese land stations (black squares) from 1996 to 1999; the gray dashed contours show the positions of the two seismic belts of the Okinawa Trough seismic zone (Font, 2002). Due to the large number of earthquakes, the size of dots are identical for all magnitudes; (b) 2075 hypocenters located by the Japan Meteorological Agency (JMA) network during the same period by using Japanese land stations (black squares); the gray dashed contours correspond to the four groups observed from the hypocenters distribution; (c) Hypocenters of 2421 microearthquakes relocated with the *simul2000* program in the southwestern Okinawa Trough for a 10-days period in 2003. All earthquakes are shallower than 60 km and their magnitude larger than 1. Legend as in Fig. 4.
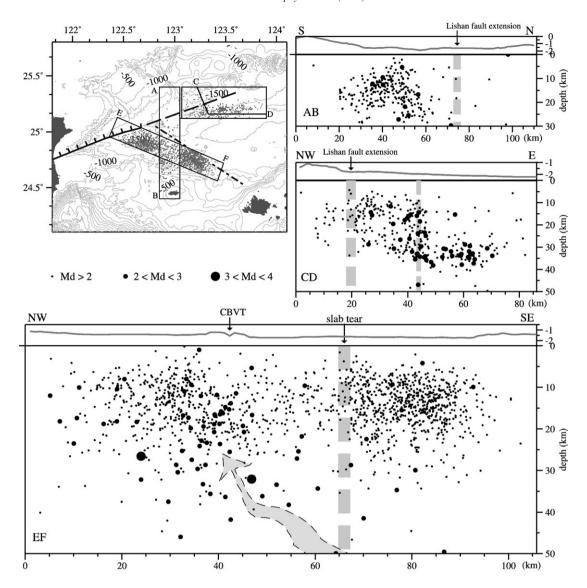
Fig. 7. In the upper left corner, general map with the position of the three cross-sections AB, CD and EF. Gray dots are the hypocenters projected on the cross-sections. The gray dashed line is the prolongation of the Lishan fault. Bathymetric contour every 500 m (Sibuet and Hsu, 2004). The hypocenters located in the three boxes are displayed in the vertical cross-sections AB, CD and EF. Black dots show the positions of hypocenters. The size of black dots is function of the magnitude. The gray dashed lines show the position of the NE–SW trending boundary on cross-section AB, of the Lishan fault extension on cross-sections AB and CD and of the slab tear (Lin et al., 2004a and b) on cross-section EF. The light arrow shows a possible conduit for fluids migration.

constrains on each side of it and decrease the backarc rifting processes in the SOT area.

3.5. Normal faulting and hypocenter distribution

In 1996, a French-Taiwanese cooperative research program (the Active Collision in Taiwan program) was carried out offshore Taiwan aboard the French research vessel R/V *l'Atalante*. More than 30 high quality seismic reflection profiles were acquired (Lallemand et al., 1997), allowing Sibuet et al. (1998) to map numerous normal faults. The locations of the normal faults determined from the seismic profiles by Sibuet et al. (1998) and Sibuet and Hsu (2004) were reported in Fig. 5 for comparison with the hypocenter distributions. Unfortunately, the error in hypocenter determinations (~3 km in plane and ~6 km in depth) and the high density pattern of active normal faults do not allow us

to associate each fault to a specific hypocenter trend. However, most earthquakes, besides those located in cluster 2, are concentrated along the E–W normal faults, and which accounts for the present-day active backarc opening process in the SOT (Fig. 5). Note that almost all the normal faults identified on the seismic profiles are active only south of the Lishan fault prolongation. This observation confirms that the main controlling factor in the SOT is normal faulting, occurring simultaneously along most of the normal faults located in the deepest part of the trough. Northwest of the Lishan fault extension, normal faulting is neither observed on seismic profiles nor recorded by the earthquake activity. This confirms that the prolongation of the Lishan fault plays a major role in the backarc opening process in the SOT area, in particular as an active transfer fault between the SOT and the area located east of the Ilan Plain and northern part of the Lishan Fault prolongation.

3.6. Vertical cross-sections of hypocenter distribution

Three vertical cross-sections are shown in Fig. 7 (AB, CD and EF). Along the N–S cross-section of hypocenters distribution (AB), the northern boundary of earthquakes is dipping north in direction of the central graben. Hypocenters presented in profile CD lie along the E–W elongated cluster 3

east of 123.45°E. Earthquakes are mostly located at a depth of 32 to 38 km. West of 123.45°E, the hypocenters distribution becomes suddenly shallower along a steep plane located in the vicinity of the 123.4°E meridian (thin gray dashed line). West of the Lishan fault prolongation (gray dashed line in cross-section CD), only a few earthquakes are observed. This sudden change in the earthquakes distribution confirms that the prolongation of
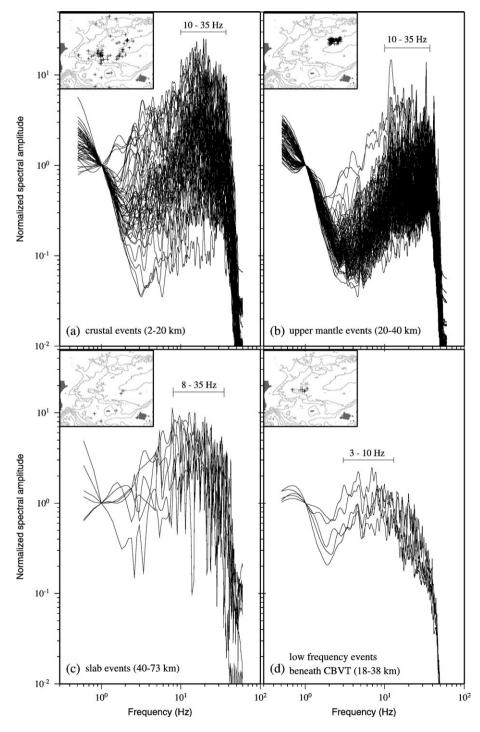

Fig. 8. Velocity spectra of P waves (a) crustal events (2–20 km); (b) upper mantle events of cluster 3b (20 to 40 km); (c) slab events (40–73 km); (d) low frequency events (18–38 km). Spectra are calculated for the initial 2 s of P waves, and spectral amplitudes are normalized at 1 Hz. Insets are general maps with location of the earthquakes used in this analysis.

Lishan fault extends to about 123.6°E meridian and forms a major crustal or lithospheric boundary, which offsets the normal faults pattern.

In cross-section EF, most of the seismicity has a crustal origin (~0–25 km). However, a cluster of earthquakes of larger magnitude is observed beneath the CBVT. Lin et al. (2004a and b) have proposed the existence of a N–S trending slab tear along the 123.2°E meridian (dashed line in cross-section EF) where an excess of H_2O-rich fluid might exist near the slab tear, increasing the melt flux. This fluid and/or melt rises through the mantle wedge in direction of the CVBT area (light arrow in Fig. 7). The interaction between the fluid and/or melt with the overlying mantle might enhance the generation of magma and give birth to a cluster of earthquakes situated just beneath the CBVT area. In other words, the origin of these earthquakes might be linked to a magmatic chamber located beneath the CBVT area. The spectrum characteristic of this cluster of earthquakes will be discussed in the later section.

4. Deep, low frequency microearthquakes

According to the seismicity distribution in northeastern Japan, most of the events occur in the upper 15 km of crust which forms the brittle seismogenic zone in the volcanic area (Zhao et al., 2002). Only a few deep microearthquakes (22–42 km) were recorded. These deep and low frequency earthquakes have been associated with an upper mantle magmatic activity (Hasegawa and Yamamoto, 1994; Hasegawa and Zhao, 1994). According to Hasegawa et al. (1991), the frequency of this type of earthquakes (low frequency events) belongs to the 0–8 Hz bandwidth compared to the 8–20 Hz bandwidth for normal crustal earthquakes. As mentioned above, some earthquakes located beneath the CBVT area originate in the upper mantle (cross-section EF in Fig. 7). To better understand the nature of this cluster, the velocity spectra have been calculated for the 2 first seconds of P-wave arrivals. In the SOT, the crustal thickness is 15–18 km (Sibuet et al., 1987). The spectra calculated for all earthquakes shallower than 20 km (crustal earthquake) give a 10–35 Hz bandwidth (Fig. 8a) in good agreement with the spectra estimated by Chang et al. (submitted for publication) with a comparable dataset. Depths of most earthquakes in the cluster 3b are larger than 20 km (20–40 km) indicating an upper mantle origin. The main frequency is also in the same 10–35 Hz range (Fig. 8b). Fig. 8c presents the spectra coming from potential slab events located at depth ranging from 40 to 73 km. The main frequency is about 8–35 Hz in a similar range than the crustal earthquakes. Fig. 8d presents the spectra calculated for the deep events beneath the CBVT area (18–38 km) (cross-section EF in Fig. 7). Their main frequency range is about 3 to 10 Hz. To summarize, the velocity spectra calculations show that the main frequency band is in the 10–35 Hz range for the earthquakes located in our study area (crustal, upper mantle and slab tectonic events), except for those situated beneath the CBVT area, where the main frequency band is in the 0–8 Hz range. The origin of these earthquakes, located beneath the volcanoes and deeper than 10 km, might be linked

to a magmatic activity as proposed for the low frequency (LF) events by Hasegawa et al. (1991). The nature of the volcanic activity beneath the CBVT area might be linked to the existence of a possible magma chamber where low frequency earthquakes are observed.

5. Results and conclusions

1. More than 3300 microearthquakes were located during the recording period of 10 days. The microearthquake activity was characterized by the ceaseless occurrence of numerous small earthquakes in the vicinity of OBS stations. Four major clusters were identified. Most of the microearthquakes are shallow and distributed along E–W trending lineaments.
2. The seismicity is restricted to the central graben area of the SOT. The earthquake occurrence ends abruptly against the NE–SW trending Lishan fault prolongation. Northwest of the Lishan fault prolongation, normal faults are absent on the seismic profiles and is not associated with earthquake activity. This confirms that the prolongation of the Lishan fault plays a major role in the backarc opening process in the SOT area and corresponds to an active transfer fault between the SOT and the northern part of the Lishan fault prolongation.
3. According to the P-wave velocity spectra analysis, the main frequency range of the normal crustal earthquakes is 10–35 Hz. For the deep and low frequency events located beneath the area of CBVT area, the main frequency range is 3–10 Hz. These low frequency events may suggest the presence of a magma chamber beneath the CBVT area.

References

Auffret, Y., Pelleau, P., Klingelhoefer, F., Crozon, J., Lin, J.-Y., Sibuet, J.-C., 2004. MicroOBS: a new ocean bottom seismometer generation. First Break 22, 41–47.
Chang, T.-Y., Sibuet, J.-C., Lee, C.-S. and Lin, J.-Y. (submitted for publication). Tremors in the Southwestern Okinawa Trough. Tectonophysics.
Chung, S.-L., Wang, S.-L., Shinjo, R., Lee, C.-S., Cheng, C.-H., 2000. Initiation of arc magmatism in an embryonic continental rifting zone of the southernmost part of Okinawa Trough. Terra Nova 12, 225–230.
Dziewonski, A.M., Chou, T.-A., Woodhouse, J.H., 1981. Determination of earthquake source parameters from waveform data for studies of global and regional seismicity. J. Geophys, Res. 86, 2825–2852.

Engdahl, E.R., Van der Hilst, R.D., Buland, R.P., 1998. Global teleseismic earthquake relocation with improved travel times and procedures for depth determination. Bull. Seismol. Soc. Am. 88, 722–743.

Font, Y., 2002. Contribution to the understanding of the westernmost Ryukyu subduction termination into the active arc-continent collision of Taiwan: new insights from seismic reflection analyses and earthquake relocation. Memoires Geosciences-Montpellier France, 244 pp.

Font, Y., Lallemand, S., Angelier, J., 1999. Etude de la transition entre l'orogène actif de Taiwan et la subduction des Ryukyu—Apport de la sismicité. Bull. Soc. Géol. Fr. 170, 271–283.

Fournier, M., Fabbri, O., Angelier, J., Cadet, J.-P., 2001. Regional seismicity and on-land deformation in the Ryukyu Arc: implications for the kinematics of opening of the Okinawa Trough. J. Geophys. Res. 106, 13751–13768.

Hasegawa, A., Yamamoto, A., 1994. Deep, low-frequency microearthquakes in or around seismic low-velocity zones beneath active volcanoes in northeastern Japan. Tectonophysics 233, 233–252.

Hasegawa, A., Zhao, D., 1994. Deep structure in island arc magmatic regions as inferred from seismic observations. In: M.P., Ryan (Ed.), Magmatic Systems. Academic Press, San Diego, pp. 179–193.

Hasegawa, A., Zhao, D., Hori, S., Yamamoto, A., Horiuchi, S., 1991. Deep structure of the northeastern Japan arc and its relationship to seismic and volcanic activity. Nature 352, 683–689.

Heki, K., 1996. Horizontal and vertical crustal movements from three-reference frame: implications for the reversal time scale revision. J. Geophys. Res. 101, 3187–3198.

Hirata, N., Kinoshita, H., Katao, H., Baba, H., Kaiho, Y., Koresawa, S., Ono, Y., Hayashi, K., 1988. Report on DELP 1988 cruises in the Okinawa Trough. Part III. Crustal structure of the southern Okinawa Trough. Bull. Earthquake Res. Inst. Univ. Tokyo 66, 37–70.

Ho, C.-S., 1986. A synthesis of the geologic evolution of Taiwan. Tectonophysics 125, 1–26.

Hsu, S.-K., 2001. Subduction/collision complexities in the Taiwan-Ryukyu junction area: tectonics of the northwestern corner of the Philippine Sea plate. Terr. Atm. Oc. Sci. 209–230 Supplementary Issue.

Hsu, S.-K., Sibuet, J.-C., Shyu, C.-T., 1996. High-resolution detection of geologic boundaries from potential field anomalies: an enhanced analytic signal technique. Geophysics 61, 373–386.

Hsu, S.-K., Sibuet, J.-C., Shyu, C.-T., 2001. Magnetic inversion of the East China Sea and Okinawa Trough: tectonic implications. Tectonophysics 333, 111–122.

Imanishi, M., Kimata, F., Inamori, N., Miyajima, R., Okuda, T., Takai, M., Hirahara, K., 1996. Horizontal displacements by GPS measurements at the Okinawa-Sakishima islands (1994–1995). Zisin 2 (49), 417–421.

Iwasaki, T., Hirata, N., Kanazawa, T., Melles, J., Suyehiro, K., Urabe, T., Möller, L., Makris, J., Shimamura, H., 1990. Crustal and upper mantle structure in the Ryukyu Island Arc deduced from deep seismic sounding. Geophys. J. Int. 102, 631–651.

Kao, H., Jian, P.-R., 2001. Seismogenic patterns in the Taiwan region: insights from source parameter inversion of BATS data. Tectonophysics 333, 179–198.

Kao, H., Rau, R.-J., 1999. Detailed structures of the subducted Philippine Sea plate beneath northeast Taiwan: a new type of double seismic zone. J. Geophys. Res. 104, 1015–1033.

Kao, H., Shen, S.-S.J., Ma, K.-F., 1998. Transition from oblique subduction to collision: earthquakes in the southernmost Ryukyu Arc-Taiwan region. J. Geophys. Res. 103, 7211–7229.

Kissling, E., Ellsworth, W.L., Eberhart-Phillips, D., Kradolfer, U., 1994. Initial reference models in local earthquake tomography. J. Geophys, Res. 99, 19635–19646.

Kubo, A., Fukuyama, E., 2003. Stress field along the Okinawa Trough and the Ryukyu Arc inferred from moment tensors of shallow earthquakes. Earth Planet. Sci. Lett. 210, 305–316.

Lahr, J.C., 1978. HYPOELLIPSE: a computer program for determining local earthquake hypocentral parameters, magnitude, and first motion pattern. USGU Open File Report, USGS, Menlo Park CA. 34 pp.

Lallemand, S., Liu, C.-S., Angelier, J., Collot, J.-Y., Deffontaines, B., Dominguez, S., Fournier, M., Hsu, S.-K., Le Formal, J.-P., Liu, S.-Y., Lu, C.-Y., Malavieille, J., Schnürle, P., Sibuet, J.-C., Thareau, N., Wang, F., 1997. Swath bathymetry reveals active arc-continent collision near Taiwan. EOS, Trans., Am. Geophys. Union 78, 173–175.

Lallemand, S., Liu, C.-S., 1998. Geodynamic implications of present-day kinematics in the southern Ryukyu. Jour. Geol. Soc. China 41, 551–564.

Lee, C.-S., Shor Jr., G.G., Bibee, L.D., Liu, R.S., Hilde, T., 1980. Okinawa Trough: Genesis of a back-arc basin. Mar. Geol. 35, 219–241.

Lee, J.-C., Angelier, J., Chu, H.-T., 1997. Polyphase history and kinematics of a complex major fault zone in the northern Taiwan mountain belt: the Lishan fault. Tectonophysics 274, 97–115.

Lienert, B., Berg, R.R., Frazer, L.N., 1988. HYPOCENTER: an earthquake location method using centered, scales, and adaptively least square. Bull. Seism. Soc. Am. 76, 771–783.

Lin, J.-Y., Hsu, S.-K., Sibuet, J.-C., 2004a. Melting features along the Ryukyu slab tear, beneath the southwestern Okinawa Trough. Geophys. Res. Lett. 31, L19607. doi:10.1029/2004GL020862.

Lin, J.-Y., Hsu, S.-K., Sibuet, J.-C., 2004b. Melting features along the western Ryukyu slab edge (northeast Taiwan) and Ryukyu slab tear (southernmost Okinawa Trough): tomographic evidence. J. Geophys. Res. 109, B12402. doi:10.1029/2004JB003260.

Lin, J.-Y., Sibuet, J.-C., Lee, C.S., Hsu, S.-K., Klingelhoefer, F., 2007. Origin of the southern Okinawa Trough volcanism from detailed seismic tomography. J. Geophys. Res. 112, B08308. doi:10.1029/2006JB004703.

Liu, C.-C., 1995. The Ilan plain and the southwestward extending Okinawa Trough. J. Geol. Soc. China 38, 229–242.

Lu, C.-Y., Hsü, K.-J., 1992. Tectonic evolution of the Taiwan mountain belt. Petrol. Geol. of Taiwan 27, 21–46.

Nakamura, M., Katao, H., 2003. Microearthquakes and faulting in the southern Okinawa Trough. Tectonophysics 372, 167–177.

Nakamura, M., Yoshida, Y., Zhao, D., Katao, H., Nishimura, S., 2003. Three-dimensional P-and S-velocity structures beneath the Ryukyu Arc. Tectonophysics 369, 121–143.

Obana, K., Kodaira, S., Mochizuki, K., Shinohara, M., 2001. Nankai earthquake dislocation area. Geophys. Res. Lett. 28, 2333–2336.

Ouchi, T., Kawakami, H., 1989. Microseismicity in the middle Okinawa Trough. J. Geophys. Res. 94, 10,601–10,608.

Sato, T., Koresawa, S., Shiozu, Y., Kusano, F., Uechi, S., Nagaoka, O., Kasahara, J., 1994. Microseismicity of back-arc rifting in the middle Okinawa Trough. Geophys. Res. Lett. 21, 13–16.

Shyu, C.-T., Liu, C.-S., 2001. Heat flow of the southwestern end of the Okinawa Trough. Terr. Atm. Oc. Sci. 305–317 Supplementary Issue.

Shyu, J.B.H., Sieh, K., Chen, Y.-G., 2005. Tandem suturing and disarticulation of the Taiwan orogen revealed by its neotectonic elements. Earth Planet. Sci. Res. 233, 167–177.

Sibuet, J.-C., Hsu, S.-K., Shyu, C.-T., Liu, C.-S., 1995. Structural and kinematic evolutions of the Okinawa Trough backarc basin. In: Taylor, B. (Ed.), Backarc Basins: Tectonics and Magmatism. Plenum, New York, pp. 343–379.

Sibuet, J.-C., Hsu, S.-K., 1997. Geodynamics of the Taiwan arc-arc collision. Tectonophysics 274, 221–251.

Sibuet, J.-C., Deffontaines, B., Hsu, S.-K., Thareau, N., Le Formal, J.-P., Liu, C.-S., 1998. The southwestern Okinawa Trough back-arc basin: tectonics and volcanism. J. Geophys. Res. 103, 30,245–30,267.

Sibuet, J.-C., Hsu, S.-K., 2004. How was Taiwan created? Tectonophysics 379, 159–181.

Sibuet, J.-C., Letouzey, J., Barbier, F., Charvet, J., Foucher, J.-P., Hilde, T.W.C., Kimura, M., Chiao, L.-Y., Marsset, B., Muller, C., Stéphan, J.-F., 1987. Backarc extension in the Okinawa Trough. J. Geophys. Res. 92, 14041–14063.

Thurber, C.H., Eberhart-Phillips, D., 1999. Local earthquake tomography with flexible gridding. Comput. Geosci. 25, 809–818.

Tsai, C.H., Lee, C.S., Wang, C., 1998. New discovery of submarine volcanoes in the westernmost part of the Okinawa Trough. Workshop for Oceanographic Research Programs Supported by National Science Council (Taiwan). 127 pp.

Tsai, Y.-B., 1986. Seismotectonics of Taiwan. Tectonophysics 125, 17–37.

Tsai, Y.-B., Wu, S.-H., 1996. On the earthquake mislocation error due to the geometrical distribution of seismograph stations in Taiwan. Proceedings of the Symposium on Taiwan Strong Motion Instrumentation Program (II), Central Weather Bureau, Taipei, pp. 178–186.

Tsumura, K., 1967. Determination of earthquake magnitude from duration of oscillation. Jishin 2 (20), 30–40.

Wang, C., Yang, M.-L., Chou, C.-P., Chang, Y.-C., Lee, C.-S., 2000. Westward extension of the Okinawa Trough and its western end in the northern Taiwan area: bathymetric and seismological evidence. Terr. Atm. Oc. Sci. 372, 167–177.

Wang, J.-H., Chen, K.-C., Lee, T.-Q., 1994. Depth distribution of shallow earthquakes in Taiwan. J. Geol. Soc. China 37, 125–142.

Wessel, P., Smith, W.M.F., 1991. Free software helps map and display data. EOS, Trans., Am. Geophys. Union 72, 441–446.

Yamano, M., Yyeda, S., Kinoshita, H., Hilde, T.W.C., 1986. Report on DELP 1984 Cruises in the Middle Okinawa Trough. IV: Heat flow measurements. Bull. Earth. Res. Inst. Univ. Tokyo, vol. 61, no. 2, pp. 251–267.

Yeh, Y.H., Lin, C.-H., Roecker, S.W., 1989. A study of upper crustal structures beneath northeastern Taiwan: possible evidence of the western extension of Okinawa Trough. Proc. Geol. Soc. China 32, 139–156.

Yu, S.-B., Chen, H.Y., Kuo, L.-C., 1995. Velocity field of GPS stations in the Taiwan area. International Symposium on Taiwan Collision, Taipei, pp. 317–327.

Yu, S.-B., Chen, H.Y., Kuo, L.-C., 1997. Velocity field of GPS stations in the Taiwan area. Tectonophysics 274, 41–59.

Zhao, D., Mishra, O.P., Sanda, R., 2002. Influence of fluids and magma on earthquakes: seismological evidence. Physics Earth and Planet. Interiors 132, 249–267.